Division of Geological & Geophysical Surveys

PRELIMINARY INTERPRETIVE REPORT 2014-1

INVENTORY AND PRELIMINARY ASSESSMENT OF GEOLOGIC HAZARDS IN THE PASSAGE CANAL–PORTAGE VALLEY AREA, SOUTH-CENTRAL ALASKA

by
Gabriel J. Wolken and Matthew S. Balazs

Northeast view of Passage Canal, one of the western fjords of Prince William Sound, south-central Alaska (June 2011). In the foreground, snow lingers on the glacier-scoured bedrock of the south side of Passage Canal. On the north side of the fjord, prominent avalanche scars and active scarps are evidence of the unstable nature of the steep, glacially-carved slopes (left). In the background (right), Billings Glacier is visible along with newly exposed terrain from its recent retreat. Photo by Gabriel J. Wolken

June 2014

CONTENTS

FIGURES

INVENTORY AND PRELIMINARY ASSESSMENT OF GEOLOGIC HAZARDS IN THE PASSAGE CANAL–PORTAGE VALLEY AREA, SOUTH-CENTRAL ALASKA

by

Gabriel J Wolken[1] and Matthew S. Balazs[1,2]

Abstract

The south-central region of Alaska is particularly susceptible to geologic hazards because of the region's complex, glacially-influenced terrain and considerable seismic activity. Many of these hazards are associated with unstable slopes that have the potential to rapidly mobilize, the result of which could be loss of life and significant damage to property and infrastructure with little or no warning. This study focuses on identifying and understanding the geologic processes that threaten the safety of people and infrastructure in the Passage Canal–Portage Valley area (including the town of Whittier), to better inform community planning, mitigation, and emergency response activities. This report is a preliminary summary of work in progress.

INTRODUCTION

Passage Canal, one of the western fjords of Prince William Sound, connects to the Portage Valley and the Turnagain Arm of Cook Inlet to the west via Portage Pass, and forms the dividing line between the Chugach Mountains to the north and the Kenai Mountains to the south (fig. 1). Portage Valley is an important transportation corridor, providing access to Portage Lake and the town of Whittier, located on the south side of Passage Canal near the head of the fjord (fig. 1). Whit-
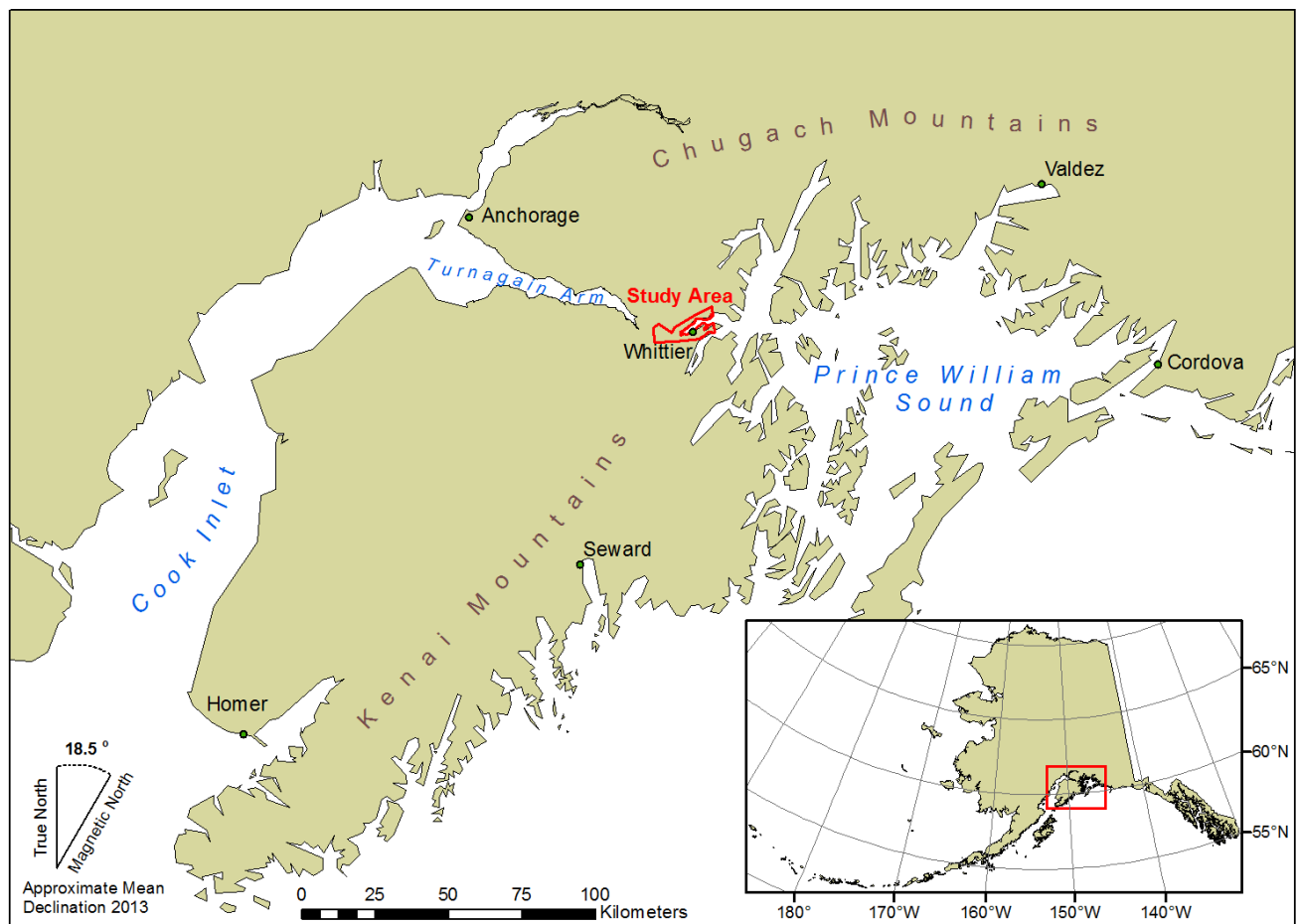

Figure 1. Map showing the study area location in south-central Alaska.

[1]Alaska Division of Geological & Geophysical Surveys, 3354 College Rd., Fairbanks, Alaska 99709-3707; gabriel.wolken@alaska.gov
[2]Department of Geology and Geophysics, University of Alaska, Fairbanks, Alaska

Figure 2. Whittier, Alaska, located near the head of the Passage Canal fjord and situated below Whittier Glacier on the subaerial part of the fan delta created by Whittier Creek. Photo by Gabriel Wolken.

tier is host to critical infrastructure for the state of Alaska; the ice-free, deepwater port is one of only two in Alaska that connects to the mainland by both rail and road (fig. 2). Earth-surface processes in the Passage Canal and Portage Valley area can threaten public safety and infrastructure and can lead to lengthy closures of important facilities and transportation routes. The economic impacts of such hazards, from the impedance of traffic in an important transportation corridor to the potential inundation of a crucial port, can be significant at local, state, and national levels. The aim of this project is to identify and understand the geologic processes that threaten the safety of people and infrastructure in the Passage Canal–Portage Valley area.

GEOLOGIC AND PHYSIOGRAPHIC SETTING

The land surrounding Prince William Sound (PWS) is characterized by high, rugged mountains up to ~4,000 m above sea level (a.s.l.) and deep, glacially-carved valleys that extend well below sea level. Numerous glaciers and several icefields occupy this complex terrain (fig. 3); they are sustained by cooler temperatures in high-elevation accumulation zones and by abundant precipitation due to their maritime location. During the Pleistocene Epoch (~2.6 million to ~11,000 years ago) numerous advances of the Cordilleran ice sheet covered the land and carved the rugged terrain of this part of Alaska (Molnia, 1986). Following the last glacial maximum (between ~25,000 and ~13,000 years ago), thick Cordilleran ice began to retreat from the region's fjords, leaving behind deeply carved, oversteepened bedrock (Kaufman and Manley, 2004). Glaciers readvanced during the late Holocene (the last ~3,000 years), with multiple phases of Little Ice Age (LIA; ~1200–1900 AD) advance recorded in western PWS. Glaciers in south-central Alaska have been in a general state of retreat for several decades and currently exhibit some of the highest glacier wastage rates on Earth (Gardner and others, 2013).

The PWS region has a maritime climate and receives abundant precipitation (liquid and solid) due to the extreme elevation gradient and proximity to the Gulf of Alaska, a region of active cyclogenesis (Aleutian low) that produces a large number of moisture-bearing storms. High-elevation areas receive heavy snow accumulation, and permafrost is likely in

Figure 3. View to southwest, Portage Pass in the foreground and Portage Lake and Portage Glacier in the background. Photo by Gabriel Wolken.

wind-scoured areas and on steep slopes where less accumulation is possible (Gruber, 2011).

The glacially-sculpted terrain of western PWS generally comprises scoured bedrock with local pockets of late Quaternary glacial, alluvial, and colluvial deposits limited primarily to valley bottoms (Bull and others, in prep.). Bedrock units in this area are dominated by the metasedimentary rocks associated with the Valdez and Orca Groups, which contribute to a thick and spatially extensive forearc accretionary complex that forms the Chugach–Prince William terrane in southern Alaska (Tysdal and Case, 1979; Nelson and others, 1985; Plafker and others, 1994). Intrusive rocks are less common in the study area, but granitic rocks associated with the Billings Glacier pluton are exposed on the north side of Passage Canal near the terminus of Billings Glacier (Tysdal and Case, 1979).

Regional tectonics strongly influenced the geology in the study area and continues to impact modern active surface processes. Passage Canal is in the northeast section of the Aleutian Megathrust, near where the Pacific and North American plates converge. This area is the source of some of the largest earthquakes in the world, and in 1964 produced North America's largest recorded earthquake (magnitude 9.2), which caused 285,000 km^2 of surface deformation and was responsible for over 100 deaths (Plafker and others, 1969).

METHODS

DATA SOURCES

Detection and identification of the geomorphological processes and landforms in the Passage Canal–Portage Valley area involved aerial- and ground-based observations and the use of a variety of remote-sensing data and geospatial analysis techniques. Remote and field-based data sources used in this study include: Medium- and high-resolution optical satellite imagery; historic aerial photographs; very-high-resolution optical aerial imagery; lidar data; Global Positioning System (GPS) data; Ground-Based Radar Interferometry (GBRI); and field observations.

High-Resolution Optical Imagery

   An aerial photographic survey of the area surrounding Passage Canal was conducted in August 2012 by DGGS scientists. The system uses a standard digital SLR camera, a GPS receiver, and a custom control box. The control box uses the time from the GPS unit to trigger an exposure of the camera at defined time intervals, allowing for consistent spacing of the photos, assuming the sensor platform (helicopter in this study) moves at a constant rate. In addition to triggering an exposure, the GPS also writes the geographic coordinates of each image to a metadata file, or EXIF file, putting the footprint of each frame into a georeferenced system.

   The aerial survey yielded more than 6,000 individual images (fig. 4), and Structure From Motion (SFM) methods were used to generate a high-resolution orthomosaic. SFM is similar to traditional photogrammetry in that it relies on overlapping pairs of images to derive positional information of the features in the images through a process of triangulation. It differs from traditional photogrammetric methods in that it does not require precise image sensor information (lens distortions), the sensor position (latitude, longitude, and elevation), or sensor orientation (yaw, pitch, roll), assuming there are sufficient ground control points in the surveyed area. The result of this survey is a high-resolution (0.10 m post spacing) orthomosaic of the area surrounding Passage Canal (Balazs and Wolken, in prep.).

Historic and Recent Imagery

   Historic and recent aerial and satellite imagery was used to analyze geomorphic change over time and assess these changes in terms of their hazard potential. The oldest dataset used (1978) consists of color infrared (CIR) photographs, scanned from the Alaska High Altitude Photography (AHAP) collection, with a spatial resolution of <1 m. An orthomosaic of these images was created using SFM methods (described above). The second dataset is from the 1996 U.S. Department of Agriculture/Chugach National Forest aerial survey. These images, Digital Orthophoto Quarter Quads (DOQQs), are part of a 1-m resolution panchromatic orthomosaic hosted by the Geographic Information Network of Alaska (GINA). The third time-stamp used was the very-high-resolution (0.10 m) orthomosaic product described in the previous section. A 2.5 m resolution SPOT-5 satellite image (2010) was used in the parts of the study area not covered by the 2012 survey.
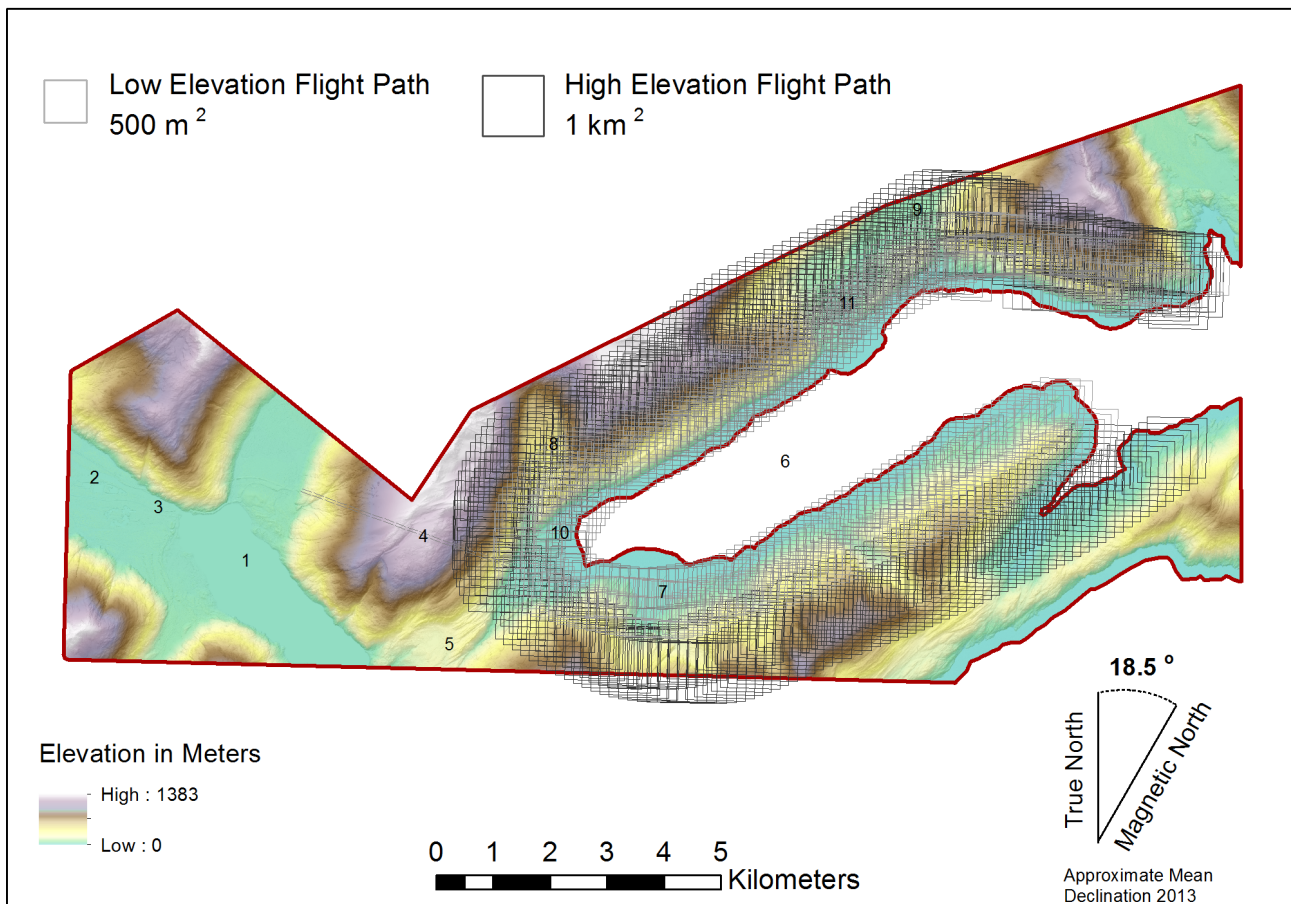

Figure 4. Image footprints from the DGGS aerial photography survey conducted in August 2012. The locations of select geographic features are labeled and include: 1. Portage Lake; 2. Portage Creek; 3. Portage Glacier Highway; 4. Anton Anderson Memorial Tunnel; 5. Portage Pass; 6. Passage Canal; 7. Whittier; 8. Learnard Glacier; 9. Billings Glacier; 10. Learnard Creek; and 11. Billings Creek.

Lidar and Derivative Products

High-resolution surface elevation data (lidar) were acquired over the study area in fall 2012. Several digital elevation model (DEM) derivative products were used to aid detection and delineation of mass movement features and slopes susceptible to snow avalanching, including hillshade, slope, variance of slope, aspect, variance of aspect, surface roughness, and curvature (methodology of McKean and Roering, 2004). While surface roughness and curvature analyses yielded little value because of the variable and extreme surface roughness in the study area, hillshade and slope products proved to be highly useful.

Ground-Based Radar Interferometry

In an attempt to delineate areas where slopes are deforming due to slumping, creep, rockfall, or sliding, and to quantify the amount of movement, we utilized a ground-based radar interferometer (GBRI). The Gamma Portable Radar Interferometer-2 (GPRI-2) transmits microwave signals in the Ku band (17.2 GHz), has a range resolution of 0.75 cm, and is able to detect movement of less than 2 mm along the look direction. Similar ground-based radar and SAR systems have been used in slope deformation studies elsewhere (Lauknes and others, 2009; Werner and others, 2012). These studies show that, by having control over the location of the sensor and the sampling frequency, the motion phases can be detected, resulting in quantifiable deformation rates of the scanned areas.

Multiple GBRI scans of Passage Canal were conducted between August 2012 and August 2013. Initial data were collected in August 2012 and serve as a reference to which all subsequent scans were compared. Additional scans were conducted following the heavy rains of October 2012 and again in August 2013. When later scans were compared to these reference sets, it was apparent that the area of interest had high coherence, indicating that deformation (i.e., slope movement) should have been detectable within the limits of the instrument (about 2 mm). However, at this time the areas and rates of slope deformation cannot be confidently reported because of low signal-to-noise ratio conditions in the data due primarily to atmospheric interference. Current and future work using this technique focuses on filtering of the atmospheric signal and capturing a longer time series.

LANDFORM AND PROCESS MAPPING

Prior to the initial field campaign (2011), study area evaluation and predictive mapping was carried out using airborne and satellite optical remote-sensing products. Orthorectified SPOT-5 data from 2010 (Geographic Information Network of Alaska [GINA], 2011) provided the most recent medium-resolution satellite imagery for the study area. Additionally, recent historical airborne data from 1982 were obtained from the Alaska High-Altitude Photography (AHAP) series. Data from these two epochs allowed for the identification of landforms associated with geologic hazards and basic evaluation of recent activity through image comparison.

Multi-day fieldwork campaigns were conducted in June 2011 and August 2012 and consisted of surveying, mapping, and landform and surface process evaluation. Ground control point (GCP) collection and horizontal and vertical measurements of specific landforms were obtained with a survey-grade GPS system consisting of two dual-frequency Topcon HiPer II GNSS receivers and an FC-250 field controller. A temporary (multi-day) static benchmark was established and processed through the National Geodetic Survey (NGS) Online Positioning User Service (OPUS). Points or features were surveyed using both real-time kinematic (RTK) and post-processing kinematic (PPK) techniques. Landform and process mapping was guided by a combination of geospatial analysis applied to high-resolution elevation data, interpretation of remote sensing data, and field ground-truthing and interpretation.

Mass Movement Inventory

A variety of methods have been developed to assess mass movement hazards (Hutchinson, 1995; Hovius and others, 1997). While the specifics between methods differ, the starting point for nearly every method is the creation of a mass movement inventory map. The reason for doing this follows the maxim that future mass movements are most likely to occur in settings where conditions are similar to those that have caused past failures (Varnes, 1984). The mass movement inventory map presented in this study is a preliminary interpretive map that combines information from historic and recent optical imagery, derivative products of a high-resolution DEM, and field observations to delineate the movement zones.

Snow Avalanche Susceptibility

The snow avalanche hazards map being generated in this study combines information from historic and recent optical imagery, derivative products of a high-resolution DEM, and field observations to delineate the zones that are susceptible to avalanching events. Avalanche indicator scars, where avalanches have damaged or stripped vegetation and debris from the slope (fig. 5), were mapped using optical imagery and field observations. However, not all avalanches cause such conspicuous vegetation scars, so the mapped areas represent only the largest and most destructive avalanche paths that have occurred in recent time. The avalanche incidence information was used to determine slope thresholds in areas interpreted to be release zones for past avalanches. The empirically derived slope thresholds (25° and 70°) are being applied to the high-resolution DEM of the study area to identify slopes that are susceptible to snow avalanching.
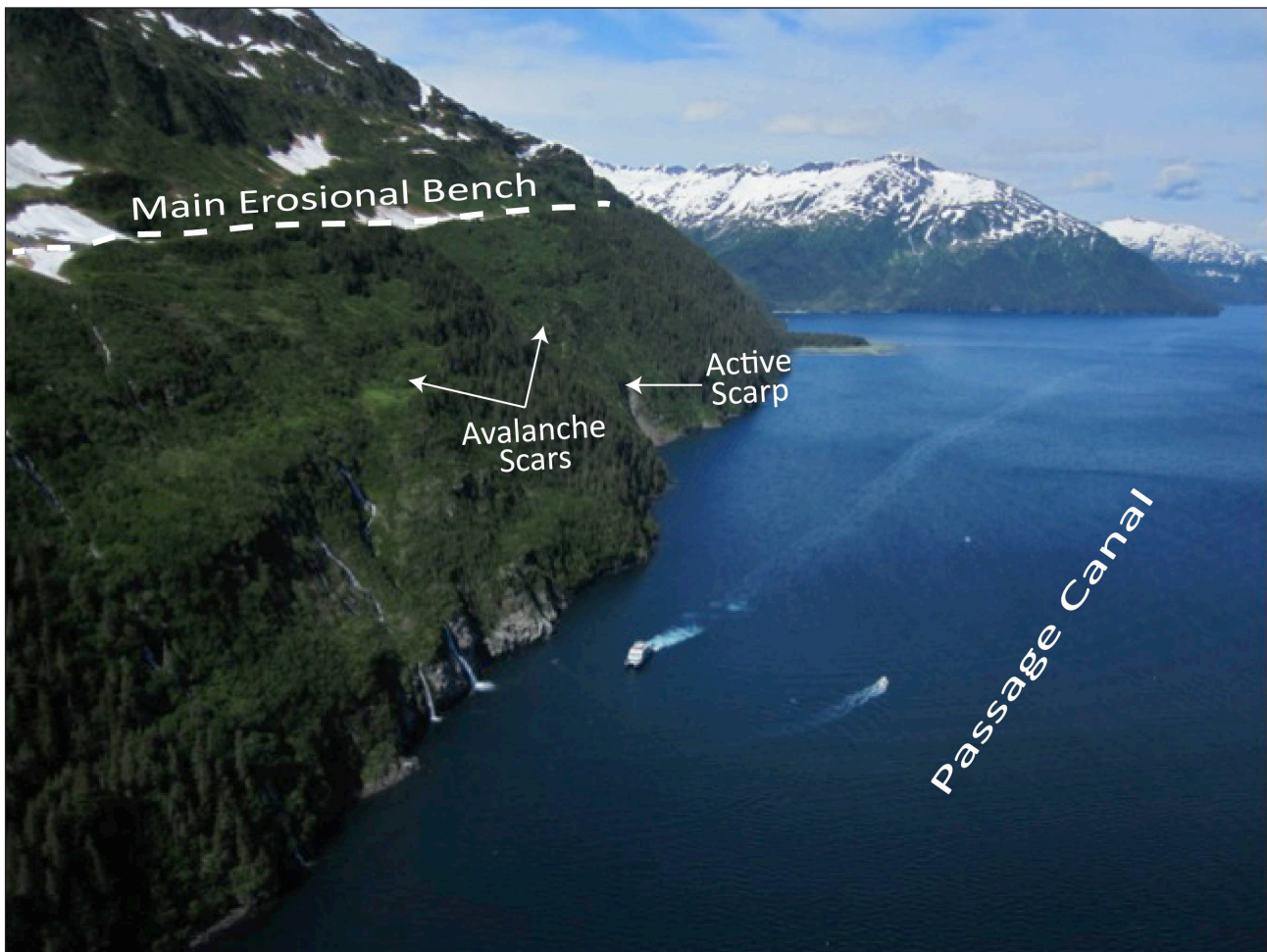
Figure 5. Photo showing the oversteepened valley wall that borders the north shore of Passage Canal. Avalanche scars and active scarps are visible in the image. Photo by Gabriel Wolken.

PRELIMINARY ASSESSMENT OF GEOLOGIC HAZARDS

CONDITIONING BY GLACIERS

Landforms in western PWS are products of the local geology and the surface processes associated with regional tectonics and climate variability and change. In this region, the processes of glaciation and deglaciation have had a dominant influence on the landscape, and have conditioned landforms and sediments for mobilization. Glaciers strongly influence the stability of slopes by eroding deep valleys and creating oversteepened sidewalls (fig. 5). While glaciers occupy a valley they exert considerable pressure on the valley walls, fracturing the bedrock. As glaciers thin and retreat, valley wall pressure is removed, leading to dilation of the surrounding bedrock and the expansion of fractures. As glaciers retreat, they also distribute erratics and drape or deposit pockets of till, often on steep or unstable slopes (Huggel and others, 2012). Such paraglacial settings are susceptible to intense thermal, mechanical, and hydraulic changes that can affect both frozen and unfrozen bedrock and glacier-derived sediments, and can strongly impact slope stability (McColl, 2012). Thermal changes, such as the warming and thawing of permafrost, are thought to be responsible for the rising number of mass movements in high-latitude and high-elevation areas (Harris and others, 2001; Gruber and Haeberli, 2007); such changes in south-central Alaska are exacerbated by high amounts of precipitation, snow avalanching, and strong ground motions caused by frequent moderate to large earthquakes.

UNSTABLE SLOPES

Unstable slopes are common throughout the study area (fig. 6). The highest concentration of mass movements occurs in northwestern Passage Canal, where the terrain has recently been deglaciated (post-LIA). Mass movements in this area are ubiquitous and multifarious, but are commonly initiated by heaving or toppling of fractured bedrock and are accompanied by large, mobile talus fields. Many of the talus fields show signs of creep or flow, depending on available moisture and slope. Areas adjacent to Learnard Glacier are highly active as a result of the interaction of multiple mass movement
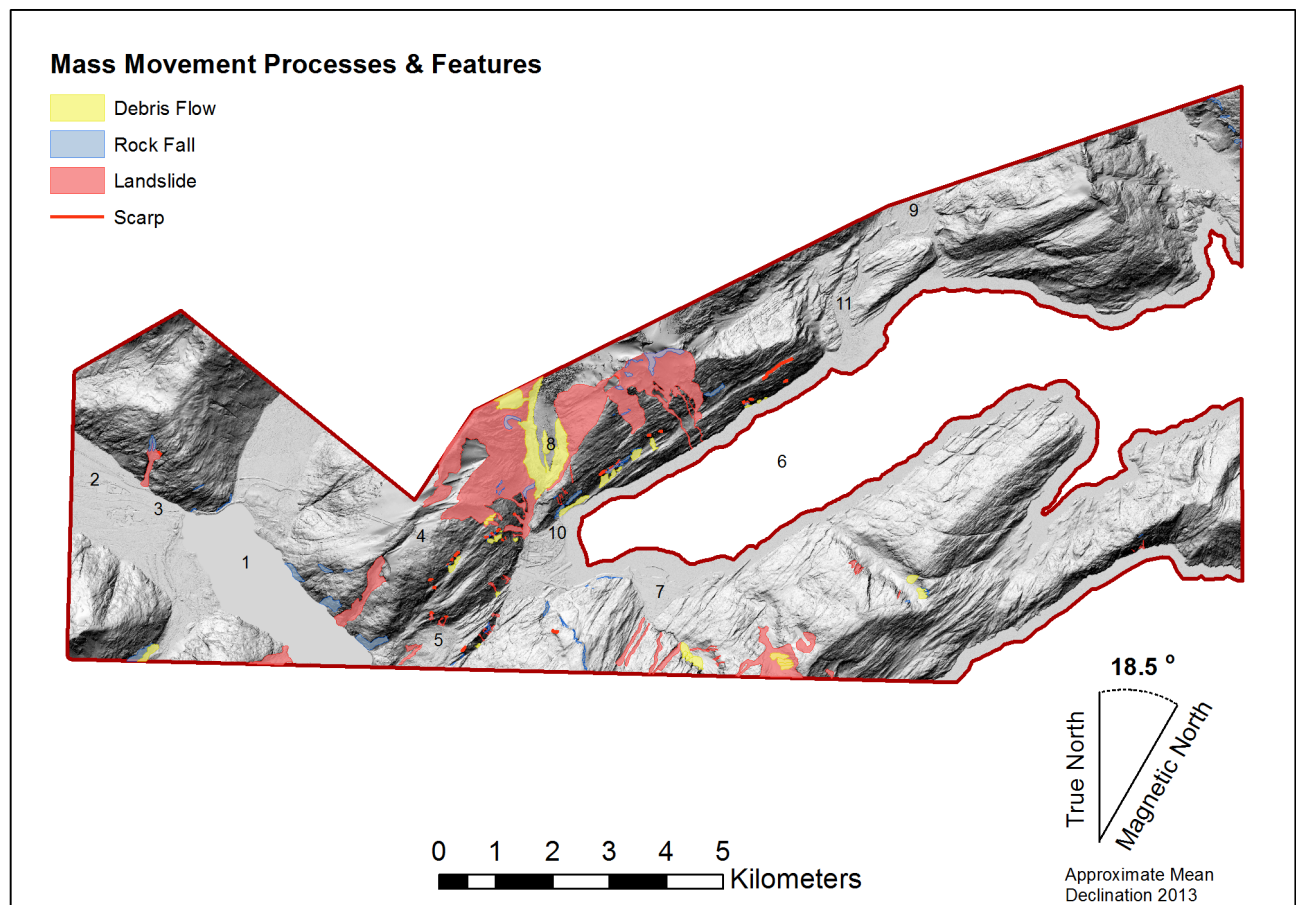
Figure 6. Preliminary map of mass movement processes and features in the study area. The locations of select geographic features are labeled and include: 1. Portage Lake; 2. Portage Creek; 3. Portage Glacier Highway; 4. Anton Anderson Memorial Tunnel; 5. Portage Pass; 6. Passage Canal; 7. Whittier; 8. Learnard Glacier; 9. Billings Glacier; 10. Learnard Creek; and 11. Billings Creek.

processes (fig. 6). For example, rockfalls originating from high-elevation localities create debris fields on or above lateral moraines deposited against the valley walls, and in some cases pockets of till exist in higher locations, perched above steep slopes. These moraines are undoubtedly ice-cored and very unstable; thermally-controlled deflation leads to unpredictable collapse of the moraine, including superimposed debris accumulated from rockfalls (figs. 7 and 8). Slope instability in this area is responsible for one known fatality in recent years (oral commun, 2014, City of Whittier).

Portage Pass and Portage Valley Slope Instability

Localized unstable slopes exist in Portage Pass and Portage Valley. In the area near the glacier-scoured apex of Portage Pass, fractured bedrock and oversteepened valley walls are highly susceptible to rockfall. Both distributed clasts and talus cones are present throughout this area, which hosts numerous hiking trails. The west side of Portage Pass transitions into recessional moraines (fig. 3), derived from the late 19th to mid 20th century retreat of Portage Glacier (Bull and others, in prep.). This till is being incised rapidly by streams draining the west side of Portage Pass; numerous debris slumps and slides exist along these stream banks where trails connect Portage Pass to the Portage Lake area.

The steep, glacier-carved valley walls surrounding Portage Lake are prone to rockfall (figs. 3 and 6). In the early 20th century, Portage Glacier occupied this valley and terminated on land near the current visitor's center. During the remainder of the 20th century, the terminus of the glacier retreated about 5 km to its present location. During this retreat, valley walls were exposed and lateral pressure, previously imposed on the walls, was removed. Countless fresh scarps, indicating the presence of active rock fall, are evident on the rock walls surrounding the lake. In the glacier-distal setting, few pockets of perched debris are identifiable along the valley walls; however, the number and size of these perched debris pockets increases near the present glacier terminus location. Much of this perched unconsolidated material can be linked to lateral moraines delineating the former height of the glacier; however, some pockets of debris appear to be suspended deposits from past landslides initiated at higher elevation. Rockfall and landslide events that enter the lake have the potential to generate large-displacement waves, creating potentially hazardous conditions for people and infrastructure both on and around the lake.
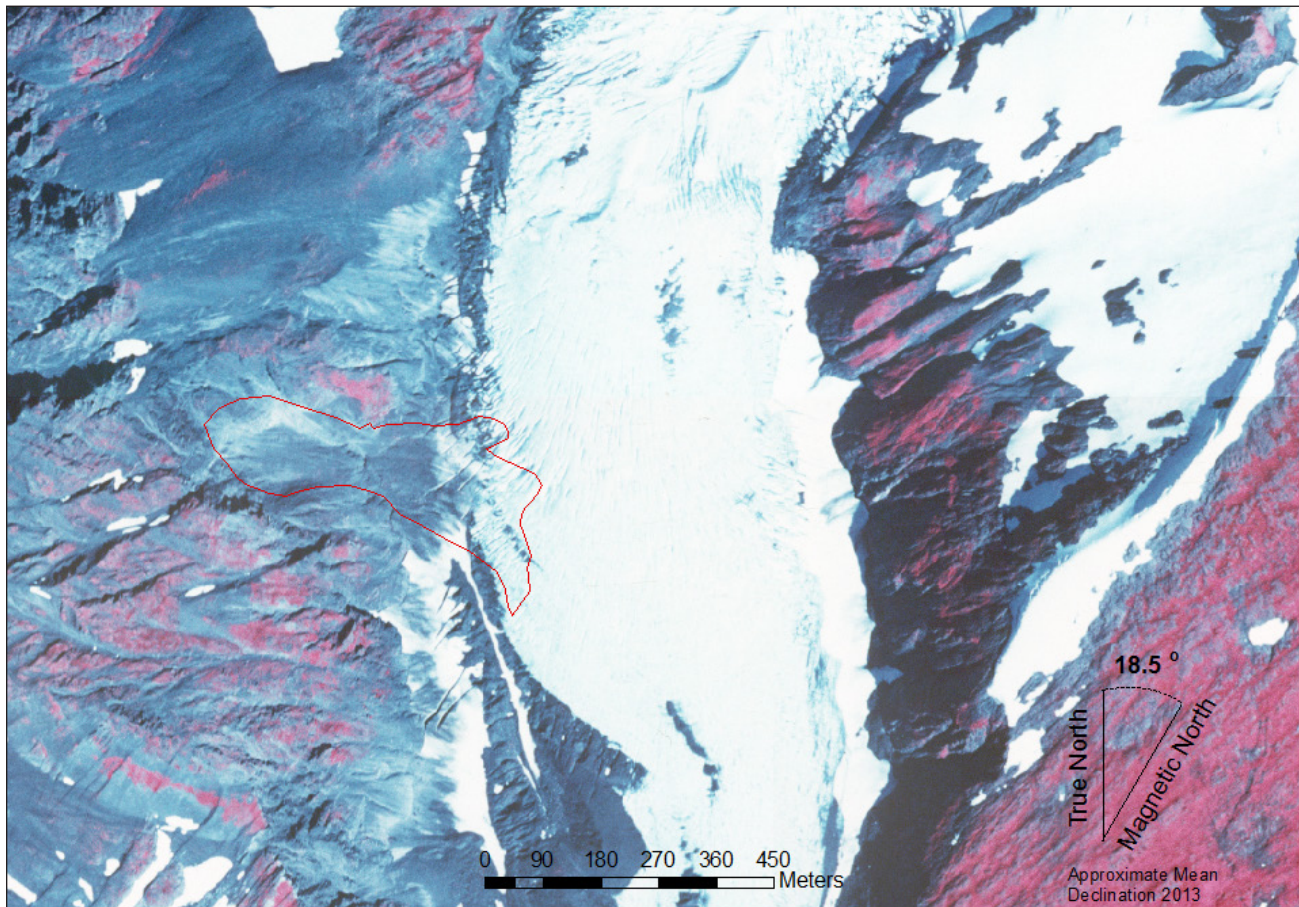
Figure 7. Orthorectified AHAP photo (1978) showing Learnard Glacier and an incipient debris flow superimposed on the west lateral moraine. Red outline shows extent of the subsequent debris flow, as mapped from 2010 imagery (fig. 8).

At the northwestern end of Portage Lake, rockfall is common along the Portage Glacier Highway between the Portage Creek crossing and the Anton Anderson Memorial Tunnel connecting Portage Valley to Whittier (figs. 6 and 9), causing hazardous driving conditions for motorists and occasional multi-day closures of the highway.

North Passage Canal Slope Instability

The alpine and subalpine slopes forming the north side of Passage Canal are highly unstable (fig. 6). From Learnard Creek to Billings Creek, numerous geomorphologic indicators provide abundant evidence of recent and historic mass movements along this section of the fjord. These indicators include fresh scarps, talus, debris slides and flows, deflating moraines, and large transported clasts. Future potential mass movements present direct hazards to marine vessels or indirect hazards to infrastructure across the fjord if displacement waves are generated (fig. 5).

The alpine area at this location is dominated by two shallow, steeply-dipping cirques that funnel debris, via fall, slide, and flow events, to lower elevation areas (fig. 10). Most of the debris from these alpine sources is deposited on a prominent erosional bench (~280 m a.s.l.) as talus and debris fans that generally coarsen downslope. Large, angular blocks (~0.6–1 m long) were found at the most distal parts of these fans, near the downslope edge of the erosional bench, providing evidence of historic high-velocity mass movement events that undoubtedly delivered debris (of similar or greater size) to sea level. Below the erosional bench, which effectively delineates the transition between alpine and subalpine areas on this otherwise continuously steep slope (~60°; figs. 5 and 6), thick vegetation masks numerous scarps formed by the structural fabric of the bedrock, glacial scour, and the post-glacial dilational response of the bedrock (figs. 11 and 12). Rockfall scarps along the north shore of Passage Canal are abundant. The largest and most active rockfall scarp, which has released blocks up to ~3.0 m long (a-axis), is located approximately 3.2 km across the fjord from Whittier. An aerial survey (2011) of this rockfall area revealed a large bedrock fracture with a downhill-facing scarp approximately 55 m (ground distance) above the active rockfall scarp (fig. 13). The fracture is mostly obscured by dense vegetation and is only visible from the air, primarily in areas of snow-avalanche scars.

Field observations of the depth of the fracture, and thus the total thickness of the block, are inconclusive. The fracture is in a broad snow-avalanche zone where rock and vegetation are regularly transported downslope. Avalanche debris are

Figure 8. Orthorectified SPOT-5 image (2010) of Learnard Glacier and a debris flow (outlined in red) that incorporated material from the west lateral moraine and traveled onto the glacier. Active slope processes dominate the Learnard Glacier valley.

lodged in the fracture, forming an intermittent false "floor" at a depth of ~2 m along the fracture's widest segments, obscuring its true depth (fig. 14). The fracture has an arcuate, convex-up form, suggesting that its origin could be related to the mechanisms influencing the active rockfall below. No other cracks are visible between the fracture and the active rockfall scarp, indicating that the bedrock block below the fracture may have detached rigidly in response to the removal of lateral support from the mountain slope (glacier debuttressing), possibly in combination with external stimuli, such as seismic activity, rapid snowmelt, or intense rainfall.

The fracture exhibits relatively less weathering and oxidation compared to surrounding rocks and remains free of vegetation, suggesting relatively recent formation or movement (fig. 14). While the age of the fracture is unknown, evaluation of historic aerial photographs indicates that the main rockfall below the fracture occurred between 1950 and 1978. It is possible that the fracture formed during the 1964 earthquake (magnitude 9.2), which was centered over PWS.

Combined ground and aerial observations, along with the analysis of lidar data acquired in fall 2012, indicate a fracture width of ~1.75–2.25 m and a length of ~160 m, with a maximum elevation above sea level of ~120 m (figs. 12 and 13). While the full length of the fracture remains unknown, the estimated surface area between the active rockfall scarp and the observed fracture is ~6,197 m^2. Based on these surface measurements and fracture depth estimates, informed by structural measurements, it is estimated that the total potential rockfall volume from this potential failure would be 1.2-1.8 million m^3, considerably less than the estimated volume of the massive rockfall (30 million m^3) that occurred during the 1958 Lituya Bay earthquake to the south (see Tsunamis section; Miller, 1960; Nicolsky and others, 2011b). Nonetheless, if mobilized, this rock mass has the potential to generate a local tsunami that could impact the community of Whittier and damage critical infrastructure in Passage Canal (Nicolsky and others, 2011b).

Although movement of the bedrock mass is largely unpredictable, monitoring the magnitude, timing, and frequency of movement can provide useful information about slope stability, independent of the effects of large-magnitude external stimuli (such as earthquake). During the summer of 2011, two monuments were installed in bedrock on the detached block below the fracture to assess its movement over time. The monuments were surveyed with high-precision GPS receivers and antennas using PPK (2011) methods (see Methods section) and reoccupied during summer 2012 using RTK solutions.

Figure 9. Rockfall debris on the Portage Glacier Highway, April 2009. Photo courtesy of the Alaska State Troopers.
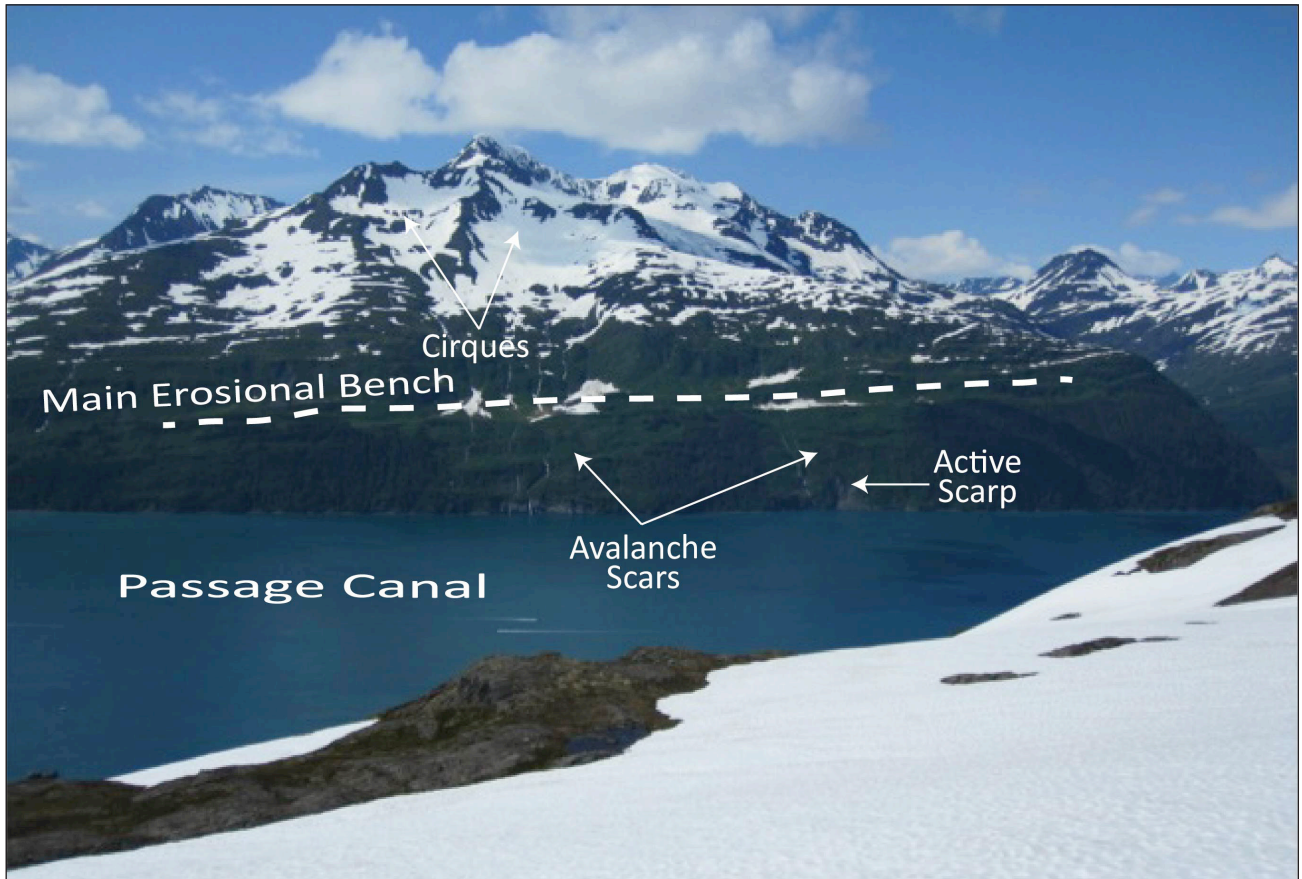

Figure 10. The glacier-carved steep terrain of the north side of Passage Canal. Photo by Gabriel Wolken.

Figure 11. High-resolution orthomosaic (2012) of a major active rockfall on the north shore of Passage Canal. The upper red line indicates a fracture in the bedrock discovered during fieldwork conducted in 2011 and the lower red line traces the top of an active scarp. Red lines in upper right of image mark other significant scarps.
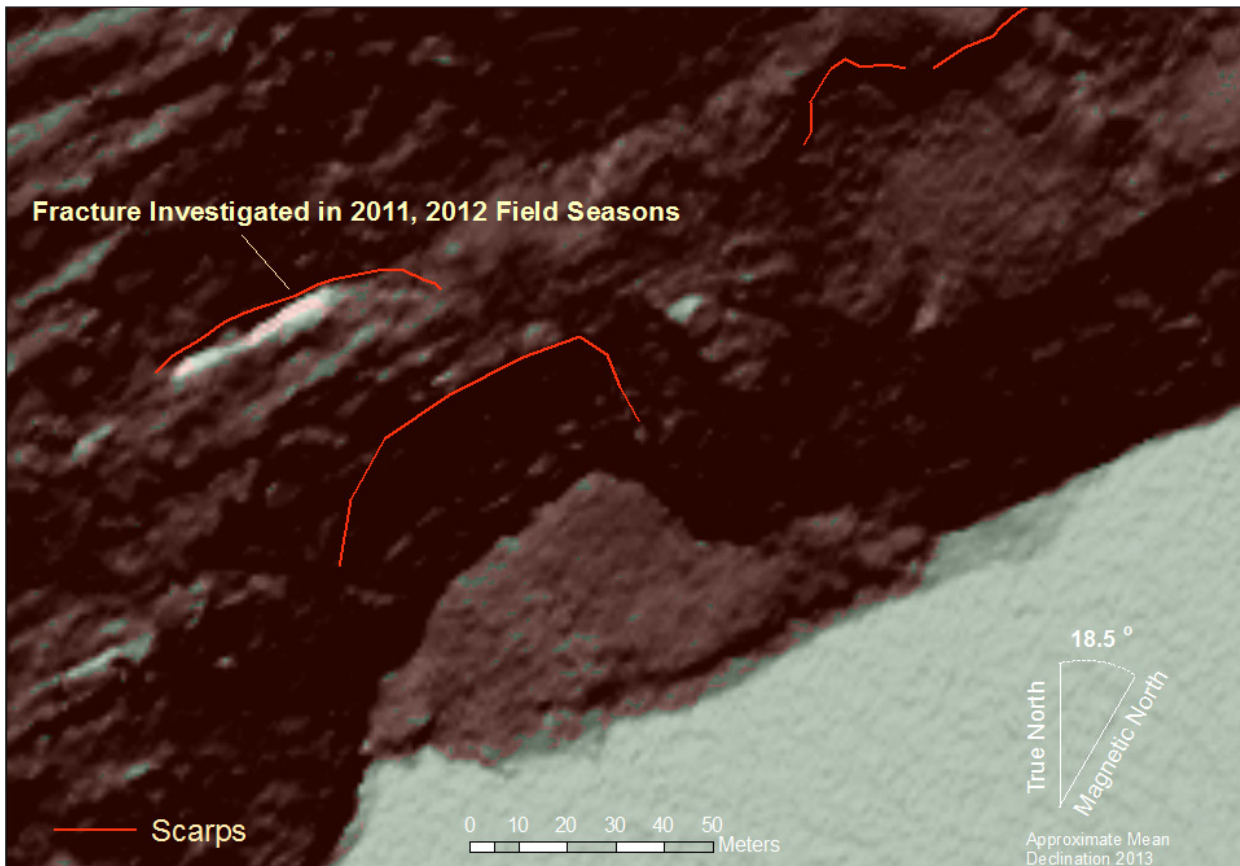

Figure 12. Bare-earth hillshade image derived from the September 2012 lidar data showing the major active rockfall on the north shore of Passage Canal. The image dimensions are the same as in figure 11. The labeled red line indicates a bedrock fracture discovered during fieldwork conducted in 2011 and the lower red line traces the top of an active rockfall scarp. Red lines in upper right of image mark other significant scarps.
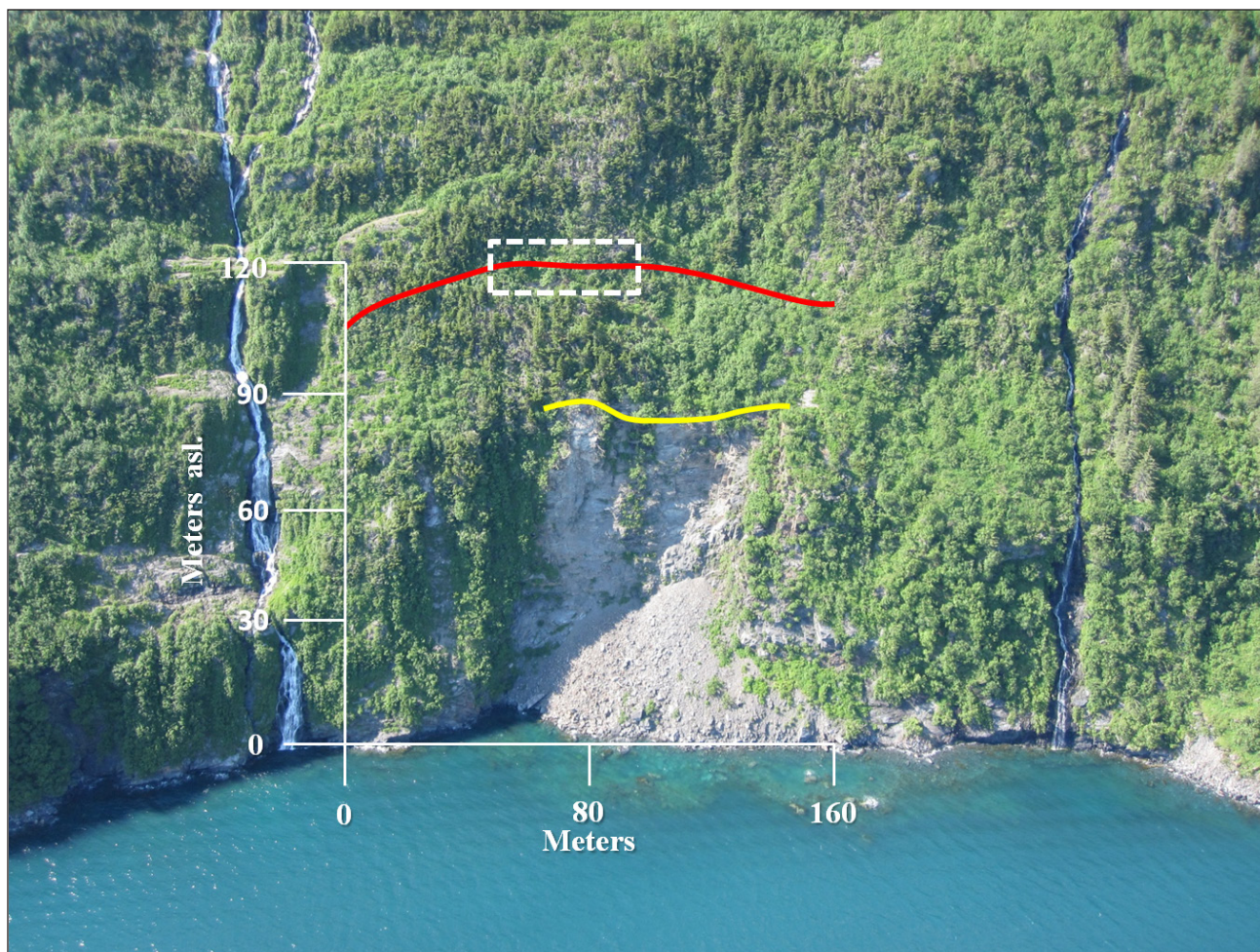
Figure 13. Photograph of the main rockfall and fracture above the north shore of Passage Canal. The yellow line shows the active scarp of the rockfall, the red line shows the position of the bedrock fracture, and the dashed white box indicates the location of the photographs in figure 14. Photo by Gabriel Wolken.

The results of the GPS analysis of monument positions between 2011 and 2012 showed a horizontal displacement of 8.5 cm (±2 cm) in the down-slope direction (115° from north), and a vertical displacement of 9.0 cm (±2 cm). The accuracy of these GPS-derived surveys depends on a number of factors, including GPS-related solution errors inherent to the technology, GPS equipment, benchmark and monument stability, and site-specific issues. The largest potential source of error (not quantifiable) is linked to the stability of the monuments between occupations, as the monuments are located in a highly active snow avalanche chute, and thus are exposed to tremendous external forces. Because of the high potential for monument stability error and the lack of multiple successive occupations, little confidence is placed on the 2011–2012 displacement measurements reported above.

SNOW AVALANCHES

Snow avalanches are a significant risk to people and infrastructure in the study area (fig. 15). The empirically derived slope thresholds used in this study define a large area of possible avalanche risk in the study area. Notable exceptions were found in the areas where slopes are less than 25°, and in areas where the structural features of the bedrock prevented snow avalanche release or reduced snow avalanche travel. The preliminary snow avalanche hazard zonation is consistent with the local climatology and the complex topography over which snow is distributed. The mean annual total snowfall for the period 1950-2011 in Whittier is 653 cm (Western Regional Climate Center 2014). Much of this annual snowfall is wet and wind-blown, allowing it to temporarily adhere to the area's steeper slopes more than the snow in mountains in a continental climate. Consequently, avalanche release zones in this area can occur on very steep slopes (up to 70°), many of which are located in high elevation areas where greater snow accumulation typically occurs.

Figure 14. Photograph of the bedrock fracture from the air (A) and the ground (B). Red arrows in A show the location of the fracture. Red arrow in B identifies a person for scale. Photo by Gabriel Wolken.

TSUNAMIS

Tsunami-inundation models of Passage Canal confirm that Whittier was impacted not only by a major tectonic tsunami produced by a distant ocean-floor displacement during the 1964 earthquake, but also by locally generated tsunamis produced by submarine landslides (Nicolsky and others, 2011a). While not as widely known or as thoroughly studied as tsunamis caused by tectonic motions during earthquakes, mass-movement-generated tsunamis can also cause loss of life and significant damage to property and infrastructure with little or no warning. Mass movements occurring above water can rapidly enter bodies of water and also produce large displacement waves. Tsunami model simulations suggest that significant inundation could result from tsunamis generated by local, potentially large, subaerial landslides, such as from mobilization of the Passage Canal fracture features (fig. 14; Nicolsky and others, 2011b). Passage Canal is particularly susceptible to mass-movement-generated tsunamis because of the fjord's complex, glacially-influenced terrain and high seismic activity (see Unstable Slopes above).

The destructive effects of mass-movement-generated tsunamis have been previously identified in south-central and southeastern Alaska. The best known and largest subaerial mass-movement-generated tsunami of historic time occurred in Lituya Bay, Alaska, on June 9, 1958, when a magnitude 7.9 earthquake occurred on the nearby Fairweather fault and produced an estimated 30 million m^3 rockfall that rapidly entered the water and initiated a tsunami with the highest wave ever recorded (524 m or 1,700 ft; Miller, 1960).

FLOODS

Like much of south-central Alaska, the Passage Canal/Portage Valley area is susceptible to flooding in response to high-magnitude runoff events. Flooding can result from intense or prolonged rainfall, rapid snow melt, rapid glacier melt, glacier lake outburst flood, and storm surge (Passage Canal). Infrastructure vulnerability to these events is greatest along the Portage Glacier Highway and in the town of Whittier. In some areas, flood potential is increased by catastrophic release of water that was temporarily dammed by active slope processes higher in the catchment. Such events are responsible for producing both damaging erosion and rapid sediment deposition.
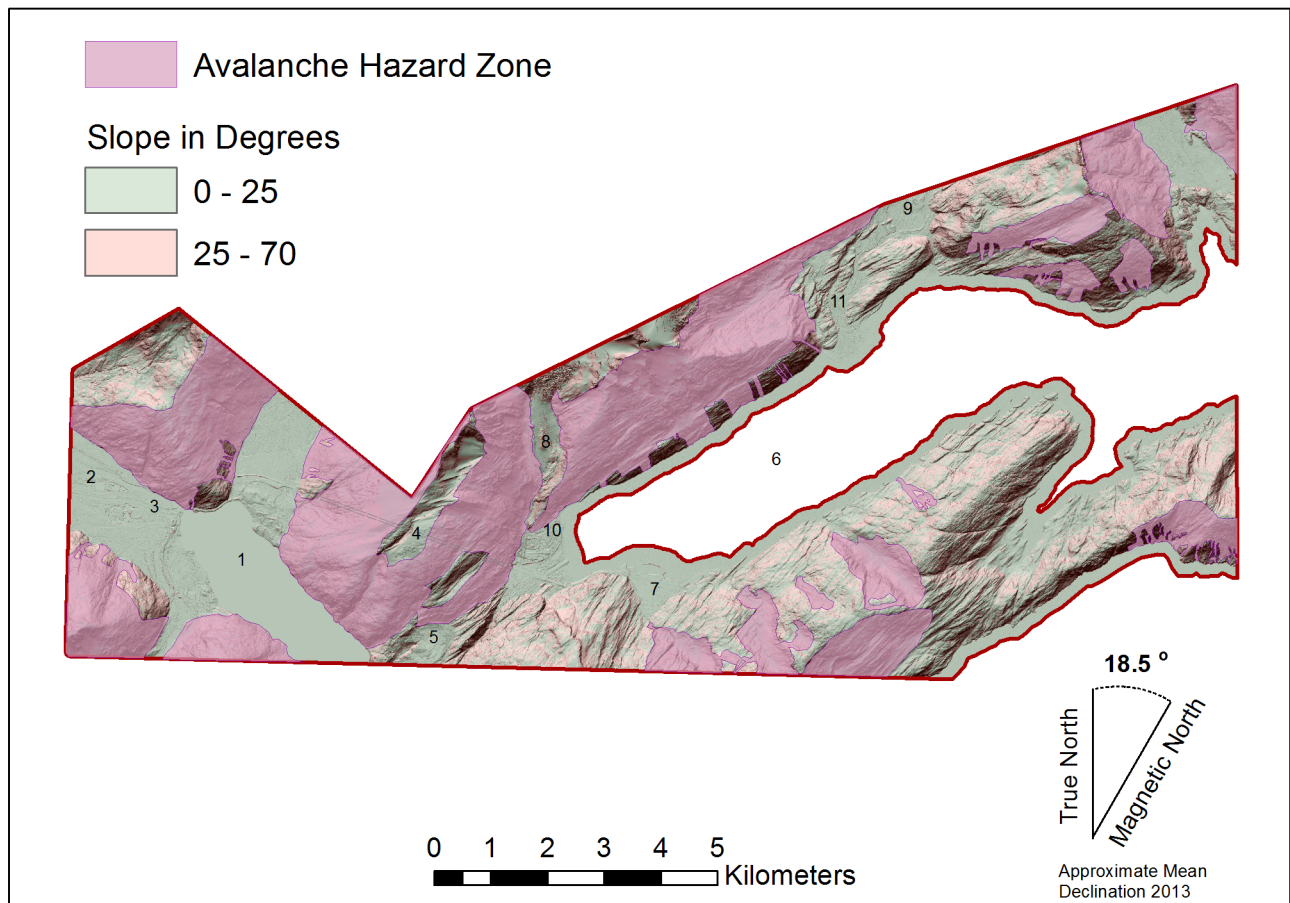
Figure 15. Preliminary map of snow avalanche hazards in the study area. The locations of select geographic features are labeled and include: 1. Portage Lake; 2. Portage Creek; 3. Portage Glacier Highway; 4. Anton Anderson Memorial Tunnel; 5. Portage Pass; 6. Passage Canal; 7. Whittier; 8. Learnard Glacier; 9. Billings Glacier; 10. Learnard Creek; and 11. Billings Creek.

CONCLUSIONS AND FUTURE WORK

Field-based observations and geospatial analyses of remote sensing data have led to the identification of multiple geological processes that threaten the safety of people and infrastructure in the Passage Canal-Portage Valley area, including the town of Whittier. This hazards inventory and preliminary assessment is part of a larger study that is focused on multi-year monitoring and more detailed hazard assessments. The results of these studies are important for assessing vulnerability to geological hazards and for informing community planners and hazards mitigation personnel.

ACKNOWLEDGMENTS

REFERENCES

Balazs, M.S., and Wolken, G.J., in prep., High-resolution orthomosaic of Passage Canal, Alaska: Alaska Division of Geological & Geophysical Surveys Report of Investigation.

Bull, K.F., Stevens, D.S.P., Gillis, R.J., Wolken, G.J., and Balazs, M.S., in prep., Geology and geologic hazards in the Whittier area, south-central Alaska: Alaska Division of Geological & Geophysical Surveys Report of Investigation.

Gardner, A.S., Moholdt, Geir, Cogley, J.G., Wouters, Bert, Arendt, A.A., Wahr, John, Berthier, Etienne, Hock, Regine, Pfeffer, W.T., Kaser, Georg, Ligtenberg, S.R.M., Bolch, Tobias, Sharp, M.J., Hagen, J.O., van den Broeke, M.R., and Paul, Frank, 2013, A reconciled estimate of glacier contributions to sea level rise—2003 to 2009: Science, v. 340, no. 6134, p. 852–857, 10.1126/science.1234532.

Geographic Information Network of Alaska [GINA], 2011, http://www.gina.alaska.edu/.

Gruber, Stephan, and Haeberli, Wilfried, 2007, Permafrost in steep bedrock slopes and its temperature-related destabilization following climate change: Journal of Geophysical Research, v. 112, no. F2, p. S18.

Gruber, Stephan, 2011, Derivation and analysis of a high resolution estimate of global permafrost zonation: The Cryosphere Discussions, v. 5, p. 1,547–1,582.

Harris, Charles, Davies, M.C.R., and Etzelmuller, Bernd, 2001, The assessment of potential geotechnical hazards associated with mountain permafrost in a warming global climate: Permafost and Periglacial Processes, v. 12, no. 1, p. 145–156.

Hovius, Niels, Stark, C.P., and Allen, P.A., 1997, Sediment flux from a mountain belt derived by landslide mapping: Geology, v. 25, no. 3, p. 231–234.

Huggel, Christian, Clague, J.J., and Korup, Oliver, 2012, Is climate change responsible for changing landslide activity in high mountains?: Earth Surface Processes and Landforms v. 37, no. 1, p. 77–91.

Hutchinson, J.N., 1995, Landslide hazard assessment, *in* Bell, D.H., ed., Landslides: Proceedings of the VI International Symposium on Landslides, Christchurch, NZ, v. 6, no. 3, p. 1,805–1,841.

Kaufman, D.S., and Manley, W.F., 2004, Pleistocene maximum and late Wisconsinan glacier extents across Alaska, U.S.A., *in* Ehlers, J., and Gibbard, P.L., eds., Quaternary Glaciations—Extent and Chronology, Part II, North America: Developments in Quaternary Science, v. 2, part B, p. 9–27.

Lauknes, T.R., Dehls, J.F., Larsen, Yngvar, and Blikra, L.H., 2009, Monitoring of the Åknes rockslide in Storfjorden, Norway, using InSAR: Fringe 2009 Workshop, ESA E SRIN, Nov. 30–Dec. 4, Frascati, Rome.

McColl, S.T., 2012, Paraglacial rock-slope stability: Geomorphology, v. 153-154, p. 1–16.

McKean, J.A., and Roering, J.J., 2004, Objective landslide detection and surface morphology mapping using high-resolution airborne laser altimetry: Geomorphology, v. 57, no. 3, p. 331–351.

Miller, D.J., 1960, Giant waves in Lituya Bay, Alaska: U.S. Geological Survey Professional Paper 354-C, p. 51–86, 1 sheet, scale 1:50,000.

Molnia, B.F., 1986, Glacial history of the northeastern Gulf of Alaska—A synthesis, *in* Hamilton, T.D., Reed, B.L., and Thorson, R.M., eds., Glaciation in Alaska—The geologic record: Anchorage, Alaska Geological Society, p. 219–236.

Nelson, S.W., Dumoulin, J.A., and Miller, M.L., 1985, Geologic map of the Chugach National Forest, Alaska: U.S. Geological Survey Miscellaneous Field Studies Map MF-1645-B, 16 p., 1 sheet, scale 1:250,000.

Nicolsky, D.J., Suleimani, E.N., Combellick, R.A., and Hansen, R.A., 2011a, Tsunami inundation maps of Whittier and western Passage Canal, Alaska: Alaska Division of Geological & Geophysical Surveys Report of Investigation 2011-7, 65 p.

Nicolsky, D.J., Wolken, G.J., Combellick, R.A., and Hansen, R.A., 2011b, Appendix B—Potential rockfall-generated tsunami at Whittier, Alaska, *in* Nicolsky, D.J., Suleimani, E.N., Combellick, R.A., and Hansen, R.A., Tsunami inundation maps of Whittier and western Passage Canal, Alaska: Alaska Division of Geological & Geophysical Surveys Report of Investigation 2011-7A, p. 45–53.

Plafker, George, Kachadoorian, Reuben, Eckel, E.B., and Mayo, L.R., 1969, Effects of the earthquake of March 27, 1964 on various communities: U.S. Geological Survey Professional Paper 542-G, 50 p.

Plafker, George, Moore, J.C., and Winkler, G.R., 1994, Geology of the southern Alaska margin, *in* Plafker, George, and Berg, H.C., eds., The Geology of Alaska: Boulder Colorado, Geological Society of America, The Geology of North America, v. G-1, p. 389–449.

Tysdal, R.G., and Case, J.E., 1979, Geologic map of the Seward and Blying Sound quadrangles, Alaska: U.S. Geological Survey Miscellaneous Investigations Series Map 1150, 12 p., 1 sheet, scale 1:250,000.

Varnes, D.J., 1984, Landslide hazard zonation—A review of principles and practice, *in* Natural Hazards, volume 3: Paris, UNESCO, International Association of Engineering Geology, Commission on Landslides and Other Mass Movements on Slopes, 63 p.

Werner, Charles, Wiesmann, Andreas, Strozzi, Tazio, Kos, Andrew, Caduff, Rafael, and Wegmuller, Urs, 2012, The GPRI multi-mode differential interferometric radar for ground-based observations, *in* Proceedings: EUSAR 2012—9th European Conference on Synthetic Aperture Radar, p. 304–307.

Western Regional Climate Center, 2014, http://www.wrcc.dri.edu/